

# The 2.5-MeV neutron time-of-flight spectrometer TOFOR for experiments at JET

M. Gatu Johnson<sup>a,\*</sup>, L. Giacomelli<sup>a</sup>, A. Hjalmarsson<sup>a</sup>, J. Källne<sup>a,b</sup>, M. Weiszflog<sup>a</sup>,  
E. Andersson Sundén<sup>a</sup>, S. Conroy<sup>a</sup>, G. Ericsson<sup>a</sup>, C. Hellesen<sup>a</sup>, E. Ronchi<sup>a</sup>, H. Sjöstrand<sup>a</sup>,  
G. Gorini<sup>c,d</sup>, M. Tardocchi<sup>c,d</sup>, A. Combo<sup>e</sup>, N. Cruz<sup>e</sup>, J. Sousa<sup>e</sup>, S. Popovichev<sup>f</sup>,  
JET-EFDA contributors<sup>g1</sup>

<sup>a</sup>Department of Physics and Astronomy, EURATOM-VR Association, Uppsala University, 75120 Uppsala, Sweden

<sup>b</sup>Department of Engineering Sciences, Uppsala University, 75121 Uppsala, Sweden

<sup>c</sup>Physics Department, Milano-Bicocca University, Milan, Italy

<sup>d</sup>Istituto di Fisica del Plasma del CNR, EURATOM-ENEA-CNR Association, Milan, Italy

<sup>e</sup>Centro de Fusão Nuclear, Instituto Superior Técnico, Associação EURATOM/IST, Av. Rovisco Pais 1, 1049-001 Lisboa, Portugal

<sup>f</sup>Euratom/UKAEA Fusion Association, Culham Science Center, Abingdon, Oxon, UK

<sup>g</sup>JET-EFDA, Culham Science Center, OX14 3DB Abingdon, UK

Received 18 October 2007; received in revised form 6 March 2008; accepted 10 March 2008

Available online 16 March 2008

## Abstract

A time-of-flight (TOF) spectrometer for measurement of the 2.5-MeV neutron emission from fusion plasmas has been developed and put into use at the JET tokamak. It has been optimized for operation at high rates (TOFOR) for the purpose of performing advanced neutron emission spectroscopy (NES) diagnosis of deuterium plasmas with a focus on the fuel ion motional states for different auxiliary heating scenarios. This requires operation over a large dynamic range, including high rates of  $>100$  kHz with a maximum value of 0.5 MHz for the TOFOR design. This paper describes the design principles and their technical realization. The performance is illustrated with recent neutron TOF spectra recorded for plasmas subjected to different heating scenarios. A true event count rate of 39 kHz has been achieved at about a tenth of the expected neutron yield limit of JET, giving a projected maximum of 400 kHz at peak JET plasma yield. This means that the count rate capability for NES diagnosis of D plasmas has been improved more than an order of magnitude. Another important performance factor is the spectrometer bandwidth, where data have been acquired and analyzed successfully with a response function for neutrons over the energy range 1 to  $>5$  MeV. The implications of instrumental advancement represented by TOFOR are discussed.

© 2008 Elsevier B.V. All rights reserved.

PACS: 52.70.-m; 29.30.Hs; 29.40.-n

Keywords: Neutron spectrometer; Time-of-flight; Fusion diagnostics

## 1. Introduction

Neutron emission from fusion plasmas carries information about the condition of neutron source, predominantly,

the reactions  $d+t \rightarrow \alpha + n$  ( $E_n = 14$  MeV) and  $d+d \rightarrow {}^3\text{He} + n$  ( $E_n = 2.5$  MeV) in DT and D plasmas, in terms of intensity and the motional state of the fuel ions, tritons and/or deuterons. The most detailed information is obtained from neutron emission spectroscopy (NES) measurements, where the main measurement figure of merit is high count rate in combination with sufficient energy resolution. This is the necessary basis for achieving sufficient statistics during short times. Time-resolved data

\*Corresponding author. Tel.: +46 18 4712797; fax: +46 18 4713853.

E-mail address: [maria.gatu@tsl.uu.se](mailto:maria.gatu@tsl.uu.se) (M. Gatu Johnson).

<sup>1</sup>See the Appendix of M.L. Watkins et al., Fusion Energy 2006, Proceedings of the 21st International Conference, Chengdu, IAEA, 2006.



given by the coordinates of the center of their area and half thickness point. This defines uniquely the coordinates of S1 as its surface is perpendicular to the axis. In the case of S2, the scintillator surfaces are perpendicular to the radius as its reference orientation. However, S2 can be tilted, which is used in the TOFOR design. The tilting (angle  $\theta$  in Fig. 1) partly compensates for the timing uncertainty introduced by variation in light propagation time to the photomultiplier (PM) tube depending on the interaction point.

In addition, special features to further enhance the achievable count rate were implemented for TOFOR:

- the S1 detector was segmented in five layers to allow for higher total event rates without running into PM tube saturation;
- specially developed PC cards were used to make dead time free recording of all detected events possible;
- the C&M system was implemented as an integrated part of the instrument to allow for corrections for any drifts from the set working points.

Optimizing the TOFOR design included balancing the conflicting requirements on efficiency and energy resolution against each other, choosing the number of detectors and determining the detectors' sizes and the solid angle coverage of the S2 in a way so as to achieve maximum detection efficiency with keeping practical construction aspects in mind. The decisions were made based on results from neutron transport simulations using the GEANT4 code [8]. The simulation results are described in detail in Refs. [7,9,10]. A 3D model of the five S1 and 32 S2 detectors of TOFOR is shown in Fig. 2. S2 was chosen to be 15 mm thick and S1 25 mm in total for the five layers (5 mm per layer) since this combination was found to maximize the efficiency at a given geometrical energy resolution of 5.8% FWHM. This constraint on the acceptable energy resolution was set considering that the total energy resolution ( $\Delta E_n/E_n$ ), including the geometrical contribution, should be on the scale of the thermal Doppler broadening for d+d neutrons from 4-keV plasmas,

i.e.,  $\Delta E/E \approx 7\%$  (FWHM using the neutron energy distribution function derived in Ref. [11]). Such an energy resolution is acceptable if the instrument can be calibrated to high accuracy and if the instrumental stability can be verified through suitable monitoring. This was, in part, provided by the specially developed C&M system. The tilting angle  $\theta$  for the S2 detectors was chosen to be  $5.0^\circ$ .

### 3. The TOFOR instrument

TOFOR was designed for installation at JET so as to view a collimated neutron flux coming up vertically from the plasma. It was built and tested as a fully assembled instrument at Uppsala University and transported to JET in parts. The design afforded disassembly and remounting within required alignment specifications. Survey and alignment performed during the construction phase were maintained when remounting at JET.

The sphere that is the basis for the TOFOR design as described above is specified by its radius (705 mm). The center of each S2 detector is placed at  $\zeta = 60^\circ$ , corresponding to a scattering angle  $\alpha = 30^\circ$  with a flight path  $L = 1221$  mm, giving a flight time  $t_{\text{TOF}} \approx 65$  ns for neutrons of  $E_n = 2.5$  MeV incoming energy.

The instrument consists of a number of different parts and subsystems. These can be divided in the spectrometer itself (consisting of the S1 and S2 detectors and the mechanical support frame), the system for DAQ and the C&M system to control and monitor the pulse response of the TOFOR detectors, including calibration stability.

#### 3.1. Instrument frame

The TOFOR support frame, made of aluminum, consists of a triangular base plate with three height-adjustable floor legs and an upper support ring with three legs attached to the base plate (Fig. 7). The base plate and ring function as the chassis for TOFOR. The chassis provides the reference for the physical mounting of the scintillators and their alignment in the TOFOR coordinate system. The origin of the coordinate system (Fig. 1) is fixed relative to the center of the base plate, whose surface is perpendicular to the system axis.

The base plate has a cylindrical hole of 150.0 mm diameter in the center, which is marked by the crossing point of the lines between four holes in the plate. A cylindrical box is placed on top of the plate to house the S1 detectors. The S1 scintillators were aligned relative to the base plate and attached to it. The box is covered with a cylindrical lid with a second hole matching the one in the base plate. The only beam-intercepting materials, apart from the S1 detector assembly, are two 0.1-mm aluminum foils at the base plate and the box lid acting as light seals.

The S2 support ring is parallel to the base plate, and thus also perpendicular to the system axis. Evenly distributed around the ring are 32 sets of machined holes for steering pins and bolt attachments for the S2 detector holders.

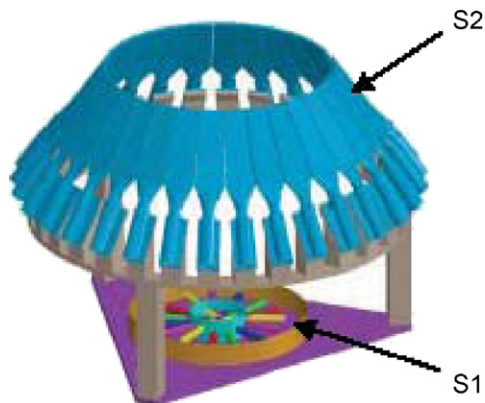


Fig. 2. Schematic of the TOFOR spectrometer showing a primary set of five S1 scintillators in the collimated neutron beam entering from below, and a secondary set of 32 S2 detectors.



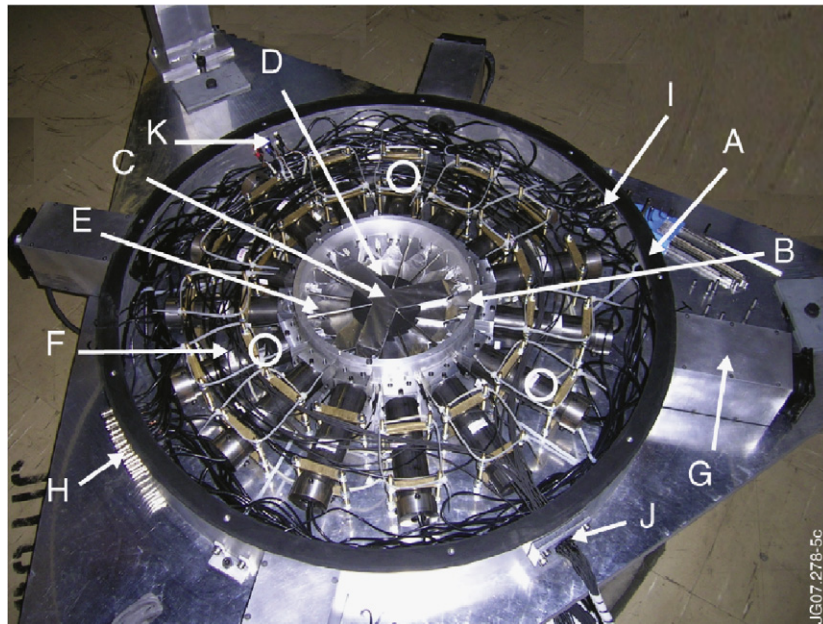


Fig. 3. Photograph of the S1 detector assembly mounted on the base plate in the outer (A) and inner (B) enclosures with the lid removed. Identified parts are (C) scintillators with light guides, (D) black cardboard, (E) light fiber guiding pipe, (F) PM holder tube, (G) cooling fan, and feed-throughs for (H) high-voltage cables, (I) signal cables, (J) optical fibers and (K) temperature probe cables (at positions indicated by circles).

The steering pin holes have a tolerance requirement of  $\pm 0.1$  mm for placing each detector at a fixed radius.

### 3.2. The S1 detector assembly

The S1 detector assembly is made up of a stack of five detector units. The detectors consist of a circular fast scintillator (Bicron BC-418<sup>2</sup>), with a diameter of 40 mm and 5-mm thickness (tolerance  $\pm 0.05$  mm). The light emission has a typical rise time of 0.5 ns and decay time of 1.4 ns. Three light guides (Bicron BC-800) are bonded to the scintillators at 120° angles to each other. These are attached, via optical silicon pads (Bicron BC-634A), to PM tubes. The PM tubes (Electron Tubes 9142A<sup>3</sup>) have a typical transient time jitter of  $< 0.6$  ns and a gain of  $10^6$  at an applied high voltage (HV) in the range 945–1145 V.

The scintillator and light-guide assemblies are wrapped in a 15  $\mu$ m layer of aluminum foil and separated by black paper to minimize light cross talk when they are placed as a stack in the inner circular enclosure of the S1 box on the base plate (Fig. 3). Each detector unit is fixed in position relative to the plate by the light guides, which rest in cradle holders in the inner enclosure wall, giving a 1-mm clearance between each layer. The lateral scintillator position is determined by clamping one light guide, while the other two are allowed free radial motion due to thermal expansion/contraction. The detectors were aligned at room temperature ( $\sim 20$  °C) relative to the base plate center to

within  $\pm 0.1$  mm. The thermal expansion would lead to a radial displacement of the scintillator center  $< 0.01$  mm/°C in different directions for the five layers (expected operating temperatures are 15–35 °C).

Each PM tube is mounted in a soft-iron pipe, also providing magnetic shielding. Each pipe is placed in a cradle attached to the base plate in such a way as to allow longitudinal motion.

Each PM tube can be fed with light pulses from the C&M system via optical fibers (Fig. 3). Guiding pipes lead the fibers through the inner enclosure to the scintillator side opposite the photocathode of the PM tube aimed at for pulsed light illumination.

The S1 box is ventilated with four fans to remove the heat produced by the PM tubes. Labyrinth ducts in the fans prevent light leaks. The temperature is monitored with three PT100 probes.

### 3.3. S2 detector assembly

The S2 detector is made of 32 modules consisting of a scintillator with attached light guide and PM tube. The plastic scintillators (Bicron BC-420) have light response characteristics in terms of rise/decay times of 0.5/1.5 ns. They are trapezoidal in shape with a thickness of 15.0 mm, length of 350 mm and top/base widths of 95.0/134.7 mm; the machining tolerance level is  $\pm 0.05$  mm. The geometrical center is used as reference to specify the position of the scintillator within the TOFOR coordinate system. The nominal angular coverage of an S2 scintillator is  $\alpha - 6.98^\circ$  and  $\alpha + 7.87^\circ$ . This means, for instance, that 2.5-MeV

<sup>2</sup>Manufactured by Saint-Gobain Crystals & Detectors, Newbury, Ohio, USA.

<sup>3</sup>Manufactured by Electron Tubes Limited, Ruislip, UK.

neutrons scattering in S1 have an energy spread from 1.53 to 2.08 MeV when they enter S2.

The scintillator base is glued to a light guide (Bicron BC-800) of fish tail shape, which changes from rectangular to circular cross-section of constant area. The scintillator–light-guide assemblies are wrapped in a  $15\mu\text{m}$  layer of aluminum foil and covered with black cardboard for light-tightness. The circular end of the light guide connects to a PM tube (Electron Tubes D671A) with the characteristics of  $<0.6\text{ ns}$  transient time jitter and a gain of  $5 \times 10^6$  at an applied HV within 1830–2230 V.

The PM tubes are mounted in soft-iron holder pipes, which also provide magnetic shielding. Each PM tube in its holder is placed in a support stand (Fig. 4) fitted to the S2 ring with steering pins and bolts to match the machined ring holes. The PM tube pipes were aligned relative to a jig so that all S2 scintillator centers ended up on the constant TOF sphere at the specified polar angle of  $\zeta = 2\alpha = 60.0^\circ$  and with the desired tilt of  $5.0^\circ$ .

The tilt was determined through combining calculated flight times for scattered 2.5-MeV neutrons from the center of S1 to different positions on S2 with test results for the S2 scintillator light transfer time obtained through character-

ization of the S2 scintillators with UV LED light (compare Ref. [12]); this limited the position-dependent spread in recorded flight times to 1 ns for 2.5-MeV neutrons. The timing results obtained from these UV LED tests on the final S2 scintillators closely match those from  $\beta$  coincidence tests done earlier on a 5 mm thick prototype with the same width and height, described in Ref. [13].

An optical fiber is directed toward each light guide through a drilled hole in the plastic collar between the soft-iron pipe and the light guide. With an angle of  $30^\circ$  to the light-guide axis, light can be transmitted to the PM tube photocathode through only one reflection. The individual fibers are connected in a light splitter on the TOFOR chassis with an ingoing fiber from the C&M system. Signal and HV cables to the electronics system are connected directly to each PM tube.

Light tightness of the individual S2 detector modules, for operation in rooms with normal light conditions, was achieved by using o-rings between the PM tubes and the holders, which were sealed with black tape to the plastic collar and the scintillator (Fig. 4).

### 3.4. DAQ electronics

The main purpose of the TOFOR DAQ system is to collect event times with maximum precision and minimal dead time. The system collects the PM tube signals from the individual S1 and S2 detectors and processes them to obtain the desired information on times  $t_1$  and  $t_2$  and deposited recoil energies  $E_{p1}$  and  $E_{p2}$  for the S1 and S2 detectors, respectively. The recoil energies are needed primarily to ensure that the right events are collected in the timing measurement. They are recorded in the form of pulse height spectra.

Three signal lines of pulse processing can be identified (Fig. 5): Line 1 for recording event times on time-digitizing (TD) boards, line 2 for recording pulse heights via analog-to-digital converters (ADC) and line 3 for counting events in scalers (ScI).

The front end of the DAQ consists of linear fan-in-fan-out (FIFO) modules of NIM standard with four inputs and four outputs per channel. The signals of the three PM tubes attached to each S1 scintillator are summed in the FIFO, while the 32 S2 detector signals are fed into separate FIFO channels. One FIFO output for each detector is fed into an ADC via a delay, and two outputs are fed into the logic circuit (LC) 1, which, in turn, provides signals to the TD (i), and to LC2 (ii and iii, Fig. 5). From LC1, there is also a branch-off leading to the scalers (branch 3a in Fig. 5). For S1, the fourth FIFO output is fed to the scalers via another FIFO for a further four-way split to count pulses above four different pulse height thresholds.

In LC1, constant fraction discriminators (CFD) convert the analog FIFO outputs above high and low threshold levels to logic pulses that are fed into programmable logic units (PLU). The CFD thresholds can be set for different operating scenarios. For instance, for typical data

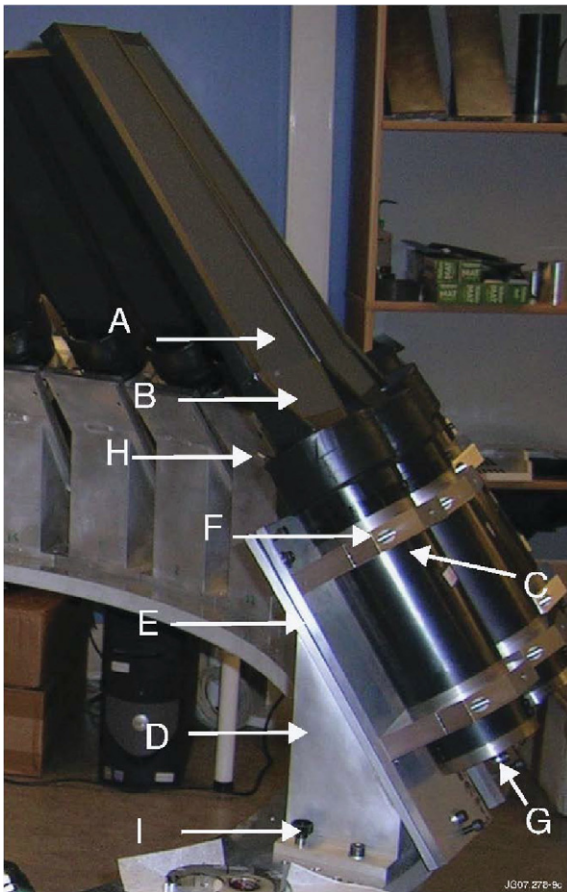


Fig. 4. S2 detector module consisting of (A) scintillator, (B) light guide, (C) PM tube soft-iron pipe, (D) support structure, (E) adjustable plate (tilting angle, direction and distance) and (F) strap holder (for longitudinal adjustment); also shown are (G) PM tube HV and signal cable connectors, (H) optical fiber access to the light guide and (I) alignment bolt.





Table 1

List of electronics modules used in the TOFOR electronics setup

Line	Module	Acronym	No. of units	Manufacturer/model
Common	Linear fan-in-fan-out	Lin FIFO	10	Caen N401, N625
Common	Constant fraction discriminator	CFD	10	Ortec CF8000
Common	Programmable logic unit	PLU	6	Caen C542
1	Time digitizing board	TD	5	IST (PCI type)
2	Logic fan-in-fan-out	Log FIFO	3	Caen N454
2	Analog-to-digital converter	ADC	3	LeCroy 4300B FERA
2	Histogram memory	Hist Mem	3	LeCroy HM413
3	Linear fan-in-fan-out	Lin FIFO	2	Philips PS748
3	Discriminator, level translator	Disc, LT	2	Caen C207
3	Scaler	SCL	2	LeCroy 4433 (ECL)
N/A	High-voltage power supply		1	Caen SY2527
N/A	HV supply board		4	Caen A1733N

threshold from LC1 for each individual detector. A level translator before the scaler provides the needed conversion from NIM to ECL signal format. The readout interval for the scalers during the acquisition period can be varied to record the data with the time resolution that suits the situation.

Scaler line 3b is used only for the five S1 detectors. The function is to monitor the PM tube gain stability during JET discharges to determine the effect of high count rates on the PM tube signal. A second set of FIFO modules is used to split the original summed S1 FIFO output signals for each S1 detector into four, which are fed into CAMAC discriminator channels with different threshold settings. The thresholds are set so that the C&M system light pulses fall in the center of the pulse height interval created. In this way, a change in pulse height due to a PM tube gain shift will be reflected in a variation in the ratio between count rate of events above different threshold levels.

The TOFOR DAQ system is linked to the JET Control and Data Acquisition System (CODAS) [16], which provides trigger signals to the DAQ and the clock input to the TDs. This is further described in Section 4.

The DAQ system is housed in three cubicles on the second floor of the JET roof laboratory. Signals from TOFOR reach the cubicles through RG 58 cables of 30 m length. The TOFOR PM tubes operate on HV supplied by a HV power supply located in the electronics cubicles and controlled via the DAQ computers. The installed PT100 temperature probes (three in the S1 box, two on the S2 detector ring and three in the electronics cubicles) are read out by PT104 readout units,<sup>4</sup> which are connected to the DAQ system in the electronics cubicles.

### 3.5. The C&M system

The TOFOR C&M system [17] is based on two pulsed light sources (PLSs), which produce light pulses of well-defined length and amplitude that can be fed into the

individual detectors. One PLS is a laser emitting 0.65-ns pulses of green light ( $\lambda = 531$  nm) at a frequency  $f \sim 5$  kHz, whose intensity can be varied through the use of a polarizer. The other is an LED emitting blue light ( $\lambda = 428$  nm). It is energized with a driver developed for TOFOR, producing 8-ns pulses of selectable frequency, typically set at 5 kHz [18]. The PLSs are placed in a separate cubicle in the roof laboratory with fiber optic runs to the TOFOR spectrometer and cable runs to the DAQ system [19]. The C&M outgoing fiber ( $\phi = 3.0$  mm) is split into a bundle of 57 individual 250- $\mu$ m fibers out of which 47 are individually connected to each TOFOR PM tube. Light pulses issued from the laser or the LED reach all detectors simultaneously (within 0.1 ns as given by the mechanical tolerance of the fiber construction).

As a calibration and stability reference for the PLS, one fiber is used to illuminate a PM tube of S1 type fitted with a small scintillator in which signals of constant pulse height are produced with a <sup>241</sup>Am  $\alpha$  source ( $\sim 3$  kBq in 2005). The PLSs are monitored for intensity drifts using this <sup>241</sup>Am absolute reference detector. The laser is typically stable to within 5% over a 1 h period and the LED to within <0.5% over a 15 h period [17].

A <sup>22</sup>Na source ( $\sim 450$  Bq in February 2005) is placed near the S1 scintillator stack in the central enclosure to allow for collection of reference pulse height spectra with distinct Compton edges, corresponding to its 511- and 1274.5-keV  $\gamma$ -lines. This information is used in order to relate the discriminator threshold settings in mV to deposited recoil energy.

### 3.6. Neutron transport model of TOFOR

As mentioned in Section 2, the TOFOR design was based on the results of extensive Monte Carlo neutron transport simulations [9]. The simulations were also used for performance evaluation, as an analysis tool and to create a detailed response function for the instrument [15].

The simulation model of the TOFOR spectrometer was created to include the scintillators themselves and other

<sup>4</sup>Manufactured by Pico Technology Limited, St Neots, UK.

relevant components with regard to composition and geometry that have an effect on neutron transport in the instrument. Neutron transport calculations were used to simulate distributions of times  $t_1$  and  $t_2$ , and deposited proton recoil energies,  $E_{p1}$  and  $E_{p2}$ , i.e., the characterizing parameters of neutron events in the individual detector elements for a given incoming neutron energy,  $E_n$ . In particular, it was determined which of the events in S1 and S2 belonged to the same neutron.

With the model, the pure geometrical response of the instrument to incoming neutron fluxes of different energies over the range of interest, typically,  $E_n = 1\text{--}5\text{ MeV}$ , could be simulated. Multiple interactions in the scintillators or the surrounding structural materials as well as scattering on carbon in the scintillators themselves were in this way accounted for in addition to the single scattering events on hydrogen in S1 and S2. The resulting  $t_{\text{TOF}}$  distributions were used to create the geometrical neutron response matrix  $R_n(E_n, t_{\text{TOF}})$ . A graphical representation of  $R_n$  is given in Fig. 6, where the interval  $E_n = 1\text{--}7\text{ MeV}$  is covered with a step length of 50 keV in the simulations and low and high threshold levels set to correspond to proton recoil energies of 0.32 and 2.30 MeV for S1 and 0.54 and 2.58 MeV for S2, respectively.

The total response  $R(E_n, t_{\text{TOF}})$  includes  $R_n$  but also the pulse response  $R_p$ , which describes how the neutron parameters  $t$  and  $E_p$  manifest themselves in the measurement, including light production, signal processing in the electronics, etc.  $R_n$  can be considered as the fundamental one with which  $R_p$  is folded in terms of some approximate function expressing the intrinsic (pulse) resolution for the time measurement as is further discussed in Section 6.

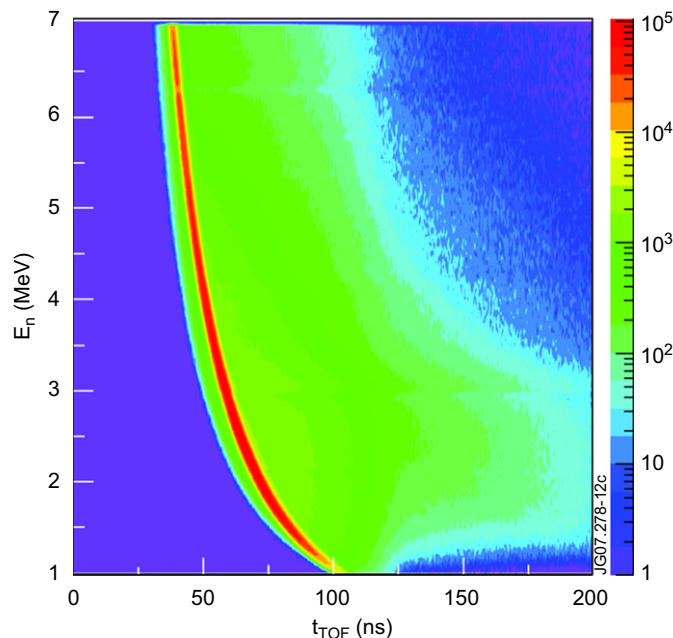


Fig. 6. Response matrix  $R_n$  for TOFOR showing the  $t_{\text{TOF}}$  spectrum as a function of simulated neutron energy  $E_n$ .

#### 4. Installation at JET and operation

TOFOR was reassembled in the JET roof laboratory in February 2005 above a 1.90 m long collimator (diameter of  $40.7 \pm 0.2\text{ mm}$ ) with respect to which it was aligned (Fig. 7). The alignment was performed with the help of a photogrammetry survey [20,21] so that the TOFOR system axis was parallel with the collimator axis (that is tilted  $0.935^\circ$  from the plumb line) to within  $0.016^\circ$ . The center of the S1 plate was measured to be  $-0.75/+0.09\text{ mm}$  away from the collimator center in the lateral  $x/y$  directions, i.e., a total radial shift of 0.76 mm. Considering the collimator geometry, this means that the entire S1 scintillator is within the collimated neutron flux. The S2 ring was surveyed to have center coordinates  $2.10/-0.24\text{ mm}$  [20] at a height of 550 mm from the base plate. The survey results show that the positioning of the instrument is well within the requirements so as to have no practical impact on the extraction of the energy distribution of the incoming neutron flux from measured  $t_{\text{TOF}}$  spectra.

The TOFOR sight line through the JET plasma is defined by the collimator through the roof laboratory floor (Fig. 8). It gives a cross-section for the maximum area of plasma viewable of  $3700\text{ cm}^2$  at the tokamak mid-plane at a distance of 19 m from the roof laboratory floor. However, this sight line is curtailed in the toroidal direction by the vertical diagnostic port on the vessel. In the radial direction, the collimator view is 40 cm wide, compared to the plasma minor radius of 1.2 m. Above the vertical diagnostic port, there is a pre-collimator consisting of two

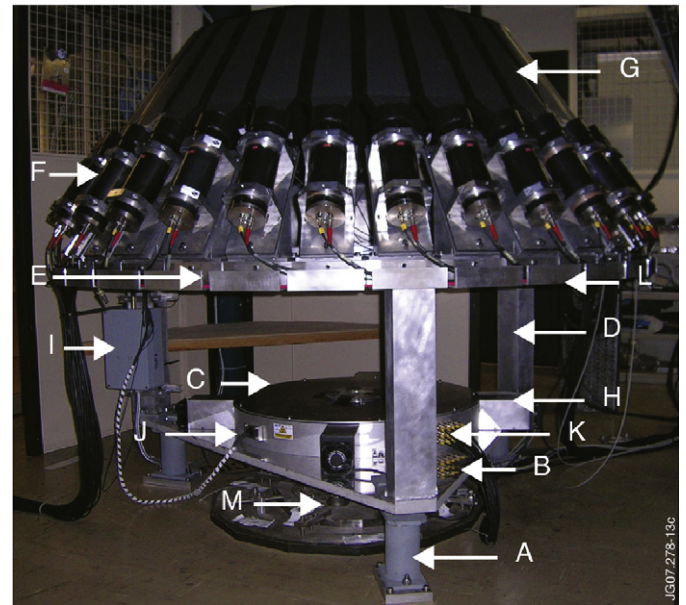


Fig. 7. Photograph of TOFOR in the JET roof laboratory with some of the main components identified: The floor legs (A), the base plate (B), the S1 enclosure (C), the legs (D), the upper support ring (E) and the S2 detector holders (F) with S2 scintillators (G). Also shown are the S1 cooling fans (H), the optical fiber connection box (I), the S1 optical fiber (J) and signal cable (K) feed-throughs and the S2 cable tray (L); (M) is the top of the neutron collimator in the roof laboratory floor.



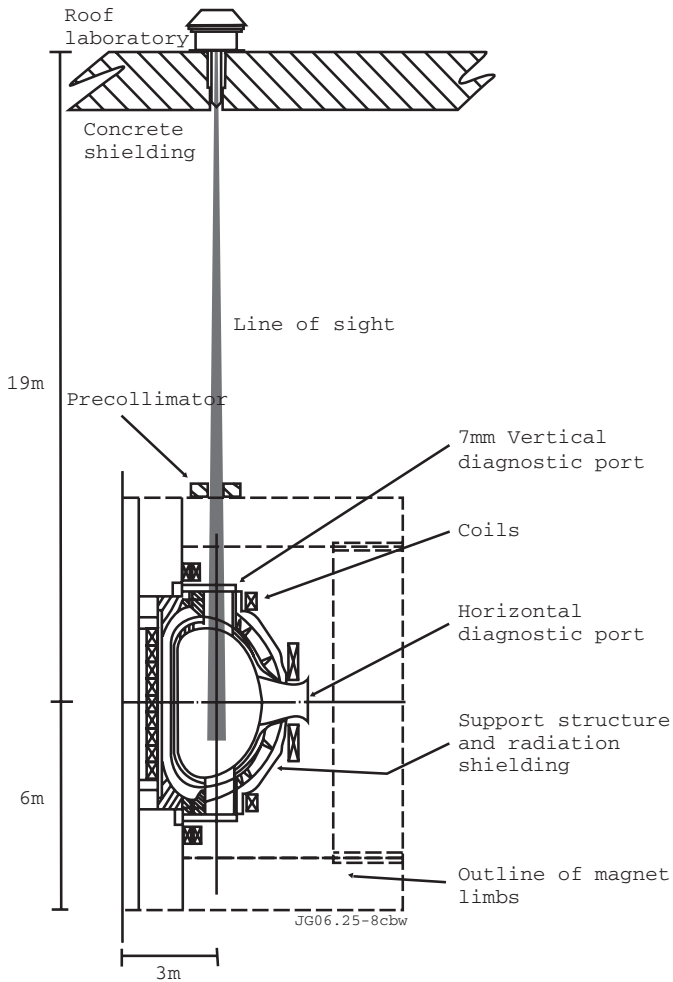


Fig. 8. Vertical TOFOR line-of-sight from the roof laboratory into the JET tokamak (poloidal cross-section) as defined by the main (1.90-m long) collimator in the concrete shielding and the size of the vertical diagnostic port. Courtesy of EFDA-JET.

pairs of jaws that are movable in the radial<sup>5</sup> and toroidal directions and that can thus be used to limit the viewed plasma volume. On their way from the plasma to TOFOR, the neutrons pass through a 7 mm thick steel plate at the port, 16 m of air, two old sets of thin metal wires in the torus hall ceiling and a 1-mm aluminum foil at the collimator base serving as gas separator between the torus hall and the roof laboratory. The flux leaving the collimator has a divergence of 10.5 mrad, which has negligible effect on the cross-section of the neutron beam through TOFOR compared to a parallel one. The parallel beam approximation was used in the TOFOR response simulations.

TOFOR is designed for observation of the collimated neutron flux  $F_n$  from JET deuterium plasmas. Typical for the observation conditions at JET is that plasma conditions undergo large variations during a discharge, spontaneously or by external controls, manifesting themselves in both yield rate and energy distribution of the neutron emission.

The expected yield rates fall in the range between  $Y_n^{\min} \leq 10^{12}$  n/s and  $Y_n^{\max} \approx 10^{17}$  n/s, corresponding to collimated neutron fluxes between  $F_n^{\min} \leq 4 \times 10^1$  n/s/cm<sup>2</sup> and  $F_n^{\max} \approx 4 \times 10^6$  n/s/cm<sup>2</sup>. Basic plasma conditions produced with Ohmic heating will have a yield rate below  $Y_n \approx 10^{13}$  n/s. High-rate plasmas are produced with the help of auxiliary heating. The TOFOR count rate response is  $C_n = 4$  kHz for  $Y_n \approx 10^{15}$  n/s. Since  $\sim 4 \times 10^3$  counts is deemed sufficient for detailed analysis, this means that time-resolved  $t_{\text{tof}}$  spectra of good quality can be collected for plasmas with  $Y_n \geq 10^{15}$  n/s, while the study of Ohmic plasmas requires long time integration periods or even summation of similar discharges to obtain desired statistics. The high count rate achievable for high yield rates affords improvement of the time resolution in the analysis, which is needed to study the fast transients that occur in plasmas with auxiliary heating.

Before plasma operation starts, TOFOR is set to certain working points, e.g., through tuning of the discriminator thresholds in LC1 (see Section 3.4). The lower threshold is rather critical (especially for S1) since it affects the admixture of multiple scattering events in the recorded  $t_{\text{TOF}}$  spectra. The TOFOR response function requires knowledge of threshold levels in units of recoil proton energy ( $E_p$  in MeV), or equivalent recoil electron energy ( $E_e$  in MeVee), while threshold levels are set in mV for pulse height. The relationship between PM tube pulse height and the corresponding recoil electron energy  $E_e$  for the individual detectors is determined by recording <sup>22</sup>Na pulse height spectra. Accurate setting of the HV is especially important for the three PM tubes on each S1 scintillator, which are summed to form a single pulse.

Another important point is the time alignment of the individual S1 and S2 detectors so that signals  $t_1$  and  $t_2$  recorded by the TD boards can be used to construct  $t_{\text{TOF}}$  spectra. For this purpose, LED pulses from the C&M system and a CAMAC TDC module with 50-ps time resolution were used. Adjustments were made with delay cables to align within 0.1 ns. This allows for addition of the individual  $t_{\text{TOF}}$  spectra without further corrections.

The running of TOFOR includes communication between the DAQ system (Section 3.4) and the JET CODAS system. Prior to each plasma discharge, CODAS sends an HTTP request to initialize the DAQ (Fig. 9). This signal triggers synchronization of the TD boards, which start collecting data as soon as the synchronization is finished. About 2 min after the initialization, the JET discharge countdown is begun via a pre-signal, which is given both as a trigger signal and as an HTTP request. The HTTP request starts the CAMAC subsystems and triggers the C&M system. The trigger signal is recorded in one of the TD channels ('clock' in Fig. 5), providing synchronization between the TOFOR DAQ system and the central JET clock. CODAS also sends two clock signals with frequencies of 1 Hz and 1 kHz, which are fed into the TD boards serving as the time calibration of the boards.

<sup>5</sup>The jaws should allow radial scan of the viewed plasma volume but this was only partially possible at the time of installation.

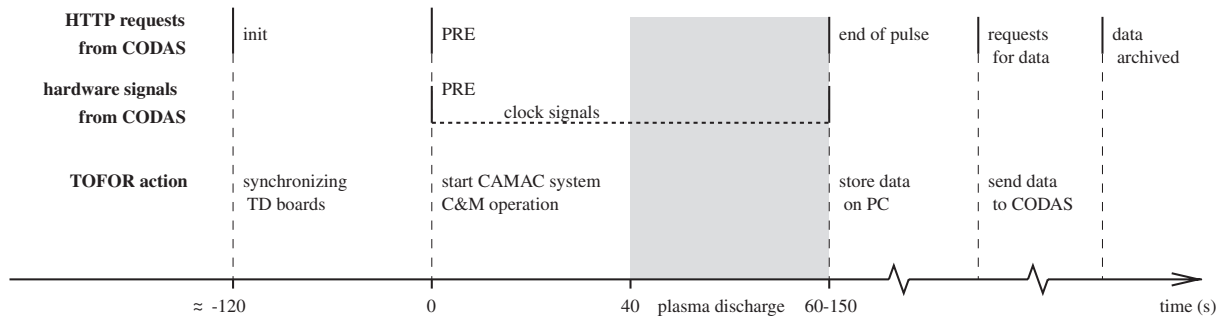


Fig. 9. TOFOR-CODAS communication signals as a function of time as part of the data recording process for JET plasma discharges. HTTP requests and trigger (hardware) signals from CODAS and their connection to TOFOR DAQ actions are indicated.

The plasma discharge starts 40 s after the pre-signal and an end-of-pulse HTTP request is sent after its completion, which triggers data transfer from all the DAQ devices to local PC storage. At some later time, CODAS sends a request for the data, which is then transferred. If all data is successfully received by CODAS, then a data archived signal is sent to the local PC and the discharge is closed. Otherwise a new HTTP request for transfer is sent.

In order to record data not connected to JET operation, TOFOR can be triggered locally. For instance, spectra from radioactive sources, ambient background radiation or C&M system signals can be recorded in this way. This feature is used for C&M functions not implemented to be performed as part of each JET discharge.

## 5. Results

The  $t_{\text{TOF}}$  spectrum is reconstructed post-discharge from the TD board time traces  $t_1$  and  $t_2$  for S1 and S2. The  $t_1$  and  $t_2$  time traces are checked for pairs within a certain time region with duration  $\Delta t_- + \Delta t_+$ , such that for every S2 event time  $t_2$  the S1 coincidences fall in  $t_2 - \Delta t_- \leq t_1 \leq t_2 + \Delta t_+$ , where  $\Delta t_{-/+}$  can be chosen arbitrarily. These time pairs can be analyzed over sequential time intervals  $\Delta t_p$  of a discharge (typically tens of milliseconds and upward) to construct the  $t_{\text{tof}}$  spectrum. This spectrum contains both accidental and true neutron coincidence pairs of S1 and S2 events, with the true ones concentrated to regions populated by fusion neutrons of say  $E_n < 7$  MeV, i.e.,  $t_{\text{tof}} > 38$  ns. Negative flight times (S2  $\rightarrow$  S1) can be recorded with TOFOR as easily as positive ones due to the time-stamping technique of the TD boards.

The level of random events per spectral channel,  $c_x$ , is constant across the  $t_{\text{tof}}$  spectrum and can be determined based on data in the region from  $t_{\text{tof}} \approx -10$  ns down to  $t_{\text{tof}} = -200$  ns. Thus, the  $c_x$  level is the measured average over some 500 channels, providing a high accuracy in the value subtracted from the measured  $t_{\text{tof}}$  spectrum to obtain a reduced spectrum representing the true coincidence rate per channel, i.e.,  $c_n = c_m - c_x$ , where  $c_m$  is the measured event rate per channel.

To illustrate the TOFOR performance, we study a  $t_{\text{TOF}}$  spectrum recorded for a plasma producing a high neutron

flux. This was achieved in deuterium discharge #69093, which was heated with neutral beams (NB) of deuterium atoms as well as radio frequency (RF) power tuned to the second harmonic resonance frequency of deuterons. The injected power was  $P_{\text{NB}} = 22$  MW, with beam energies  $E_b = 80$  and 130 keV, and  $P_{\text{RF}} = 6$  MW, giving a neutron yield rate of  $Y_n = 1 \times 10^{16}$  n/s.

The spectrum shown in Fig. 10A is based on data accumulated during the plasma time interval  $t_p = 46.0$ –48.5 s (i.e.,  $\Delta t_p = 2.5$  s) of the discharge. At  $t_{\text{TOF}} \approx 4$  ns, there is a small peak due to gammas (in the few MeV range) in the beam from the plasma, which scatter in S1 and arrive 4.1 ns later in S2. This gamma peak provides a consistency check for the TOFOR time calibration. The broad spectrum from  $t_{\text{TOF}} \approx 50$  ns and upward is due mostly to true neutron coincidences. The random background is constant over the shown interval  $-200$  to  $200$  ns. The average random level is determined from the time interval  $-200 \text{ ns} < t_{\text{TOF}} < -10$  ns as described above. One obtains a value of  $n_x = 160$  counts per channel, corresponding to a random rate of  $c_x = n_x / \Delta t_p = 64$  Hz per channel. After subtraction of the random events, a reduced  $t_{\text{TOF}}$  spectrum is obtained, the positive  $t_{\text{TOF}}$  part of which is shown in Fig. 10B. The subtraction of  $n_x$  eliminates the events in the  $t_{\text{TOF}} < 40$  ns region apart from the gamma peak and the statistical scatter.

The coincidence count rate in the reduced spectrum is  $C_n = 39$  kHz within the selected TOF window,  $0 \text{ ns} \leq t_{\text{TOF}} \leq 200$  ns. The spectrum is dominated by the peak at  $t_{\text{TOF}} \approx 65$  ns, which corresponds to single scattering neutron events of energies  $E_n \approx 2.5$  MeV, while multiple scattering events give a tail toward higher  $t_{\text{TOF}}$ .

The TOFOR measurements can also be illustrated in terms of count rates as functions of plasma time  $t_p$ . The single rates of the S1 and S2 detectors  $C_1(t_p)$  and  $C_2(t_p)$ , for discharge 69093 discussed above, are presented in Fig. 11.

Here, one can note that  $C_1(t_p)$  for S1 starts at a low level in the 50 Hz range up to  $t_p \approx 44.5$  s, reflecting the plasma conditions with Ohmic heating only, which it returns to for  $t_p > 52$  s. The intermediate region of higher rates, with a plateau at the 1 MHz level from  $t_p = 45$  to 52 s, is due to enhanced neutron yield rate caused by the application of auxiliary heating. The time trace  $C_2(t_p)$  for S2 shows the

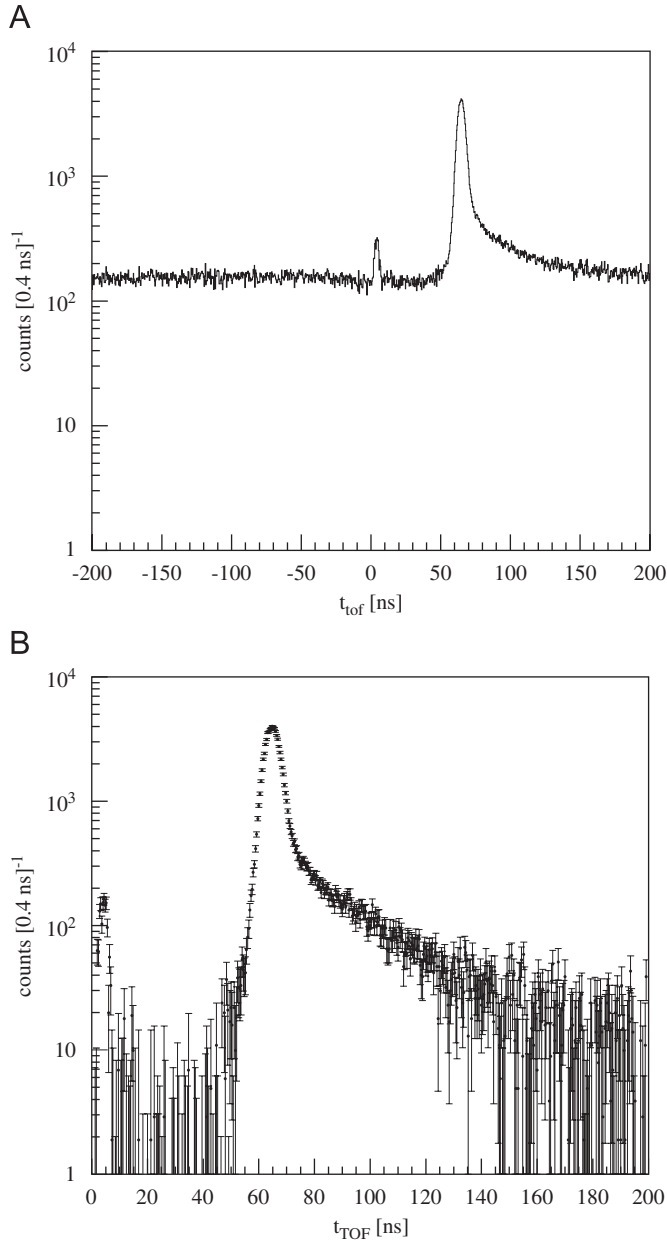


Fig. 10. Measured  $t_{\text{TOF}}$  spectrum using TOFOR to observe the neutron emission from a JET plasma (#69093) of deuterium heated through NB and RF power injection. Shown are the data before (A) and after (B) subtraction of admixed accidental events.

same general trend, but for a higher constant rate level before and after the heating period. This is due to ambient background radiation to which S2 has a higher sensitivity than S1 in proportion to its greater scintillator volume (a factor of  $10^3$ ).

Below, some examples illustrating how the measured  $t_{\text{tof}}$  spectra are used to extract information on the energy distribution of the incoming neutron flux are given. The first example is JET discharge #68396, a NB-heated deuterium plasma with a power of  $P_{\text{NB}} = 7.0$  MW injected with 130-keV beams. The NB power creates a neutron source of a quasi-steady state lasting about 9 s at a yield

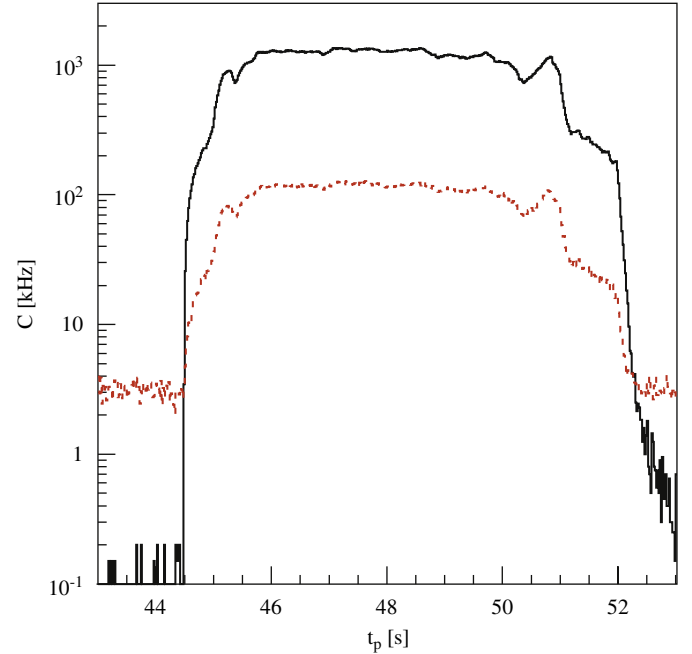


Fig. 11. Summed measured single rates as functions of elapsed plasma time  $t_p$  for the five S1 and 32 S2 detectors of TOFOR for discharge #69093 (top solid and bottom dashed curves,  $C_1(t)$  and  $C_2(t)$ ). The results were obtained with the time digitizer cards using a time binning of 20 ms.

rate of  $Y_n = 1.5 \times 10^{15}$  n/s, resulting in a TOFOR count rate at the  $C_n = 6.3$  kHz level. The measured  $t_{\text{tof}}$  spectrum (integrated from 44.5 to 53.5 s of the plasma discharge) was determined to have an average accidental admixture of  $n_x = 14$  counts per channel, which was subtracted to obtain the reduced  $t_{\text{tof}}$  spectrum (Fig. 12A).

This spectrum was compared with the predicted  $t_{\text{tof}}$  distributions obtained from an assumed incident neutron spectrum  $F_n(E_n)$  folded with the response function  $R(E_n, t_{\text{tof}})$ . From the parameterized model for  $F_n(E_n)$ , one produces a trial spectrum, which is varied to give the best fit to the measured  $t_{\text{tof}}$  spectrum, with the result presented in Fig. 12B. The trial spectrum consists of a thermal component, representing neutrons from reactions between two fuel ions in thermal equilibrium, and a beam component, representing reactions between one beam and one thermal ion. In addition, a backscatter component, representing the energy-degraded neutrons that scattered off the reactor walls before detection in TOFOR, is needed to accurately describe the data [22]. The thermal component is modeled with a Gaussian and the beam component using a half-box slowing down distribution; for further details concerning the modeling see Ref. [23]. The shape of  $F_n(E_n)$  is fairly well established in this case; hence the achieved good description of the data lends credit to the instrumental performance and the adequacy of the matrix  $R$  of TOFOR.

Another example is discharge #69529 subjected to RF heating, specifically, ion cyclotron resonance heating coupling to the second harmonic frequency of deuterons in



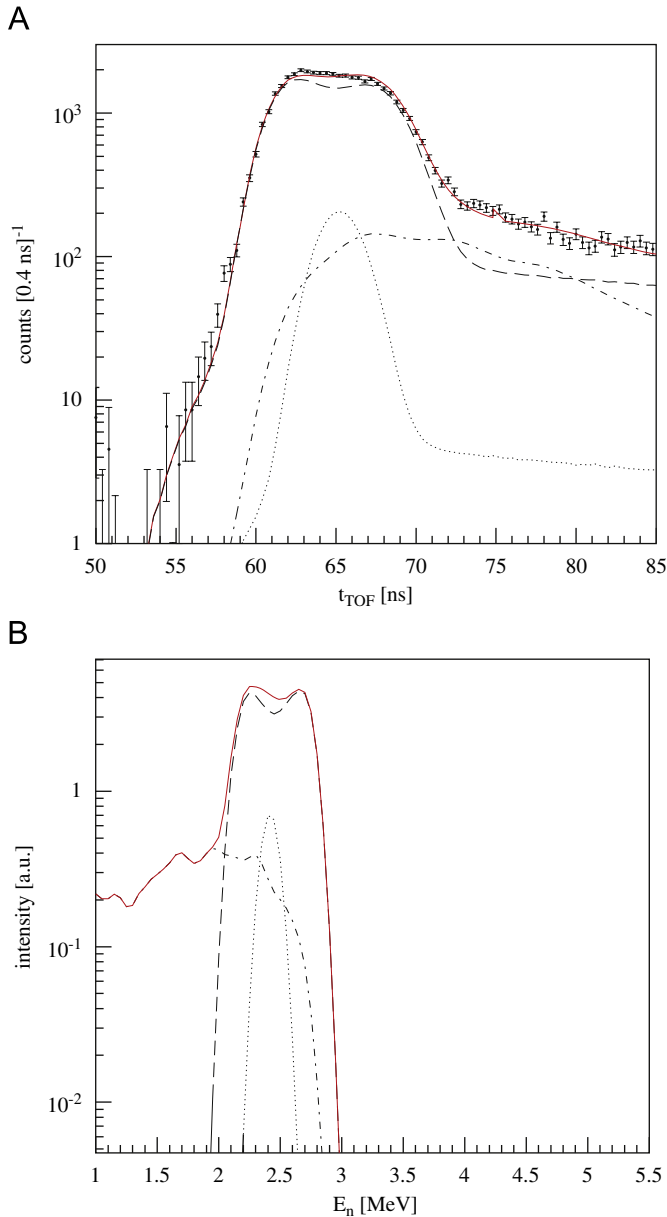


Fig. 12. (A) Example of reduced  $t_{\text{of}}$  spectrum obtained with TOFOR for the neutron emission from a JET deuterium plasma (#68396) with NB power injection. The dotted curve represents the thermal component, the dashed curve the beam component, the dash-dot curve the admixture of backscattered neutrons and the solid curve (that follows the measurement points) represents the summed fit. (B) Neutron spectrum extracted from the data in (A) using a least-squares fitting. Again the dotted curve is the thermal component, the dashed curve the beam component, the dash-dot curve the admixture of backscattered neutrons and the solid curve the summed fit.

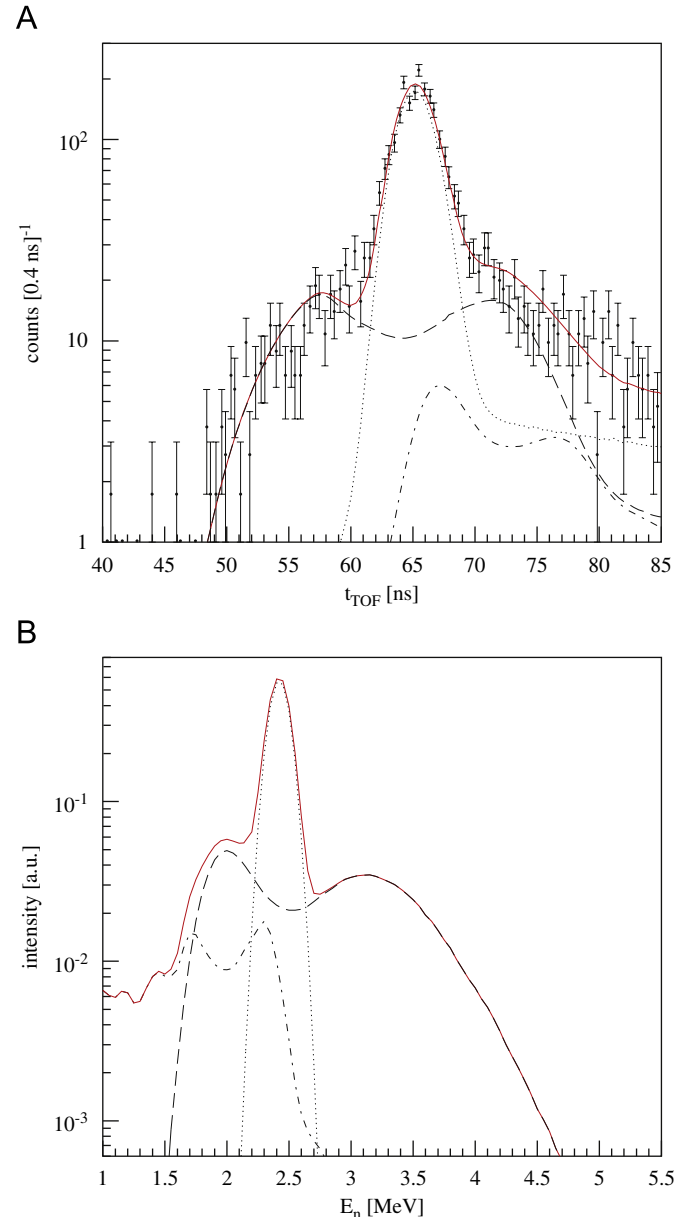


Fig. 13. (A) Example of reduced  $t_{\text{of}}$  spectrum obtained with TOFOR for the neutron emission from a JET deuterium plasma (#69529) with RF power injection. The dashed curve represents the RF component, the dotted curve the thermal component, the dash-dot curve the admixture of backscattered neutrons and the solid one (that follows the measurement points) the summed fit. (B) Neutron spectrum extracted from the data in (A) using a least-squares fitting. Again, the dashed curve represents the RF component, the dotted the thermal component, the dash-dot the admixture of backscattered neutrons and the solid curve the summed fit.

the plasma center. The effect is typically their acceleration to high energies, i.e., temperatures of the order 100 keV compared to the bulk deuterons of a few keV. The high-energy deuterons produce neutrons with a large energy spread when they fuse with bulk deuterons. The result is a  $t_{\text{of}}$  spectrum (Fig. 13A), integrated from 50 to 60 s of the plasma discharge, which is much wider than that for NB injection (Fig. 12A). It can be well

described with a predicted  $t_{\text{of}}$  spectrum using the neutron spectrum shown in Fig. 13B, with a thermal, an RF and a backscatter [22] neutron component. The thermal component again represents neutrons from reactions between ions in thermal equilibrium, and the RF component reactions between one thermal and one RF-heated ion. The model used for the thermal component is again a Gaussian. The RF component is modeled

based on a perpendicular Maxwellian deuterium distribution (see Ref. [23]).

In this case, the neutron spectrum is found to have a significant amplitude over an extended energy range from about  $E_n = 1.7$  to 4 MeV. The region of interest in the  $t_{\text{tof}}$  data ranges from below  $t_{\text{tof}} \approx 50$  to about 80 ns (Fig. 13A). The observation of RF-heated plasmas is, therefore, a test of TOFOR as a broadband neutron spectrometer.

## 6. Discussion

The aim set for TOFOR was to exploit fully the high flux from JET deuterium plasmas and translate it into high count rate  $C_n$ . To this end, the count rate capability  $C_n^{\text{CAP}}$  should be sufficient to allow operation of TOFOR up to the maximum JET neutron flux, while TOFOR should be capable of operating over the full dynamic range  $D = F_n^{\text{max}}/F_n^{\text{min}} = 4 \times 10^6/4 \times 10^1 = 10^5$  discussed in Section 4 if sufficient integration time is allowed. The efficiency required to reach high count rates should be balanced against a desired energy resolution for 2.5 MeV neutrons of order 7% FWHM. Moreover, plasmas produce neutrons with a significant energy spread (typically 1 to >5 MeV), which requires a spectrometer with matching bandwidth.

The volumes of the S1 and S2 scintillators need to be large to reach high flux detection efficiency and, hence, count rate; this also means that S2 should provide maximum coverage of the solid angle for neutrons scattered from S1. On the other hand, the volumes must be limited to avoid too high admixture of multiple scattering events in the measured  $t_{\text{tof}}$  spectrum relative to those due to neutrons that only scattered once in S1 and once in S2. A volume limit was also set by the required  $t_{\text{tof}}$  resolution for given  $E_n$  belonging to the neutron response function  $R_n$ . From the optimization simulations with the GEANT4 code, it has been determined that the flight path variations relative to the constant TOF sphere geometry (Fig. 1) contribute  $[\Delta E_n/E_n]_{R_n} = 5.8\%$  to the energy resolution for 2.5 MeV neutrons with a flux efficiency value of  $\varepsilon = 0.12 \text{ cm}^2$  [9]. This is the instrumental resolution that one would observe for mono-energetic neutrons of  $E_n = 2.5$  MeV apart from the finite resolution by which the times  $t_1$  and  $t_2$  for events in S1 and S2 can be measured, i.e.,  $[\Delta E_n/E_n]_{R_p}$ . Although  $R_p$  is complex, it can, to lowest order, be assumed to be independent of  $E_p$  [10]. When represented with a Gaussian distribution, a value of  $[\Delta t_{\text{TOF}}]_{R_p} = 1.5 \text{ ns}$  (FWHM) has been estimated based on preliminary measurements at JET [23]. An intrinsic time resolution of 1.5 ns gives a contribution of  $2(1.5/65) = 4.6\%$  to the total energy resolution  $\Delta E_n/E_n = 7.4\%$  (FWHM). This Gaussian approximation has been used for  $R_p$ , as part of  $R$ , to describe and analyze the measured  $t_{\text{tof}}$  spectra in experiments at JET to illustrate the TOFOR performance. The resolution should be compared to the set target of  $\sim 7\%$ .

A central aspect for the performance is count rate capability,  $C_n^{\text{CAP}}$ . This depends on the acceptable upper

limit on the ratio between accidental events and true coincidences in the selected region of the measured  $t_{\text{tof}}$  spectrum, i.e., the ratio  $C_x/C_n$ . The accidental event rate is directly related to the single rates in S1 and S2, i.e.,  $C_x = C_1 C_2 \Delta t_C$ , where  $\Delta t_C$  is the selected time region. The random level can be controlled and reduced by accepting only desired events, for instance, through pulse height discrimination. This is most effectively applied to  $C_1$ . In TOFOR, it is done by eliminating events that are kinematically incompatible with np scattering into S2. As all count rates increase with the incoming neutron flux, i.e.,  $C_x \propto F_n^2$  and  $C_n \propto F_n$ , one obtains  $C_x/C_n \propto F_n$ . In other words, the random contribution increases linearly with the flux, meaning that weak contributions to the spectrum will be harder to distinguish at higher count rates.  $C_n^{\text{CAP}}$  is also limited by the fact that single rates must not exceed the rate limit of individual PM tubes. The single rates in S2 are lower; hence this is most critical for the in-beam detector, S1, which is therefore split into five scintillator units to improve its performance at high rates [9]. Both the single rate and the  $C_x/C_n$  limitations are closely related to the capabilities of the DAQ system.

The stability of the TOFOR TOF spectrum is regularly monitored with the integrated C&M system. The time scale of the spectrum is given by a zero point (determined through recording of LED pulses) combined with the TD board bin width of 0.4 ns. The contribution to the uncertainty from the bin width is found to be negligible when double-checking against the JET clock pulses. The zero-point contribution is  $\sim 0.4$  ns. This leads to an indetermination in the derived neutron energy spectrum due to the calibration of the time spectrum on the single percent level for 2.5 MeV neutrons.

Calculations indicate that spectroscopy of components on the few percent level is possible for count rates of about 40 kHz with a time resolution of  $\Delta t_p = 2.5$  s. For weaker components, the neutron flux has to be decreased and longer data collection times are required. On the other hand, the main peak can be analyzed at count rates of  $C_n = 400$  kHz with a time resolution of  $\Delta t_p = 0.25$  s and a statistical accuracy better than 2%.

To be able to deduce the spectral broadening and thus the plasma ion temperature,  $C_x/C_n$  at half the peak amplitude should not exceed 1:1. From these numbers, an upper limit for the TOFOR count rate capability of  $C_n^{\text{CAP}} = 500$  kHz is deduced. At this count rate level, the single rates in the individual S1 layers also approach their capability limit.

## 7. Conclusions

TOFOR is a spectrometer to perform advanced neutron emission spectroscopy (NES) diagnosis of deuterium plasmas in magnetic confinement. The instrument implements the two scintillator detector systems S1 and S2, with the latter covering a large area of a sphere that allows the energy distribution of the incoming neutron flux to be

determined from the measured flight time ( $t_{\text{tof}}$ ) distribution. A C&M system with new PLS is implemented to assist in the calibration and verification of the instrumental stability. The times of events in S1 and S2 are measured with dedicated PC cards that allow continuous recording and storage of data for entire JET discharges lasting up to tens of seconds. The spectrometer response to neutrons was modeled to determine the  $t_{\text{tof}}$  spectrum for arbitrary energies in the typical range 1–5 MeV, or higher with reduced sensitivity. The response simulations give a detailed description of the single and multiple scattering contributions to the  $t_{\text{tof}}$  spectrum, which is the basis for extracting information on the incoming neutron spectrum.

The performance of TOFOR has been demonstrated in measurements at JET. While TOFOR is optimized for neutrons around 2.5 MeV, good NES results have been extracted for a bandwidth from 1 to >5 MeV. TOFOR has been operated successfully at count rates up to 40 kHz when JET operated at a yield rate of 1/10 of its expected maximum of  $Y_n = 10^{17}$  n/s. The results obtained indicate a count rate capability limit of about 0.5 MHz, which could be approached in future JET experiments. The data taken with TOFOR at JET show that the  $t_{\text{tof}}$  spectra recorded for different neutron emission conditions are described by the response function and the analysis model. Thus, the results obtained from the analysis are taken as a demonstration of the level of confidence that can be placed in the NES diagnostic results.

TOFOR, with the new DAQ, has demonstrated great versatility as exemplified by the measurement of the  $t_{\text{tof}}$  neutron spectra for different plasma conditions at JET. Moreover, it also allows one to reduce the admixture of accidentals in the measurement, besides making accurate correction thereof. The new DAQ system has contributed to raising the count rate capability of TOF instruments in NES diagnosis of fusion plasmas by more than an order of magnitude.

With the TOFOR instrument it is now possible to perform NES diagnosis of deuterium plasmas with considerably higher quality of data than has been previously possible. The target set for TOFOR to reach the same NES diagnostic capability for D plasmas that has been previously demonstrated by other types of instruments for DT plasmas has been achieved.

## Acknowledgments

This work has been performed under the auspices of European Fusion Development Agreement and the Association EURATOM-VR (Sweden). It has been financially supported as the JET Enhancement project on Contract EFDA JET/CSU# JW1-EP-DIAG.TOFOR, the

Swedish Research council (VR), Uppsala University, Milano-Bicocca University, and Institute of Plasma physics (CNR), Milano.

## References

- [1] G. Ericsson, et al., *Rev. Sci. Instr.* 72 (2001) 759.
- [2] T. Elevant, *Nucl. Instr. Meth. A* 476 (2002) 485.
- [3] O.N. Jarvis, *Nucl. Instr. Meth. A* 476 (2002) 474.
- [4] J. Källne, et al., *Phys. Rev. Lett.* 85 (6) (2000) 1246.
- [5] G. Gorini, J. Källne, *Rev. Sci. Instr.* 63 (10) (1992) 4548.
- [6] A. Hjalmarsson, et al., *Rev. Sci. Instr.* 72 (2001) 841.
- [7] A. Hjalmarsson, et al., *Rev. Sci. Instr.* 74 (2003) 1750.
- [8] S. Agostinelli, et al., *Nucl. Instr. Meth. A* 506 (2003) 250.
- [9] A. Hjalmarsson, et al., Neutron transport simulations for the design and performance optimization of the TOFOR neutron time-of-flight spectrometer, Uppsala University Neutron Physics Report UU-NF 05#12, December 2005, ISSN 1401-6269, <http://www.inf.uu.se/Reports/Internal.html>.
- [10] A. Hjalmarsson, Development and construction of a 2.5-MeV neutron time-of-flight spectrometer optimized rate (TOFOR), Ph.D. Thesis Acta Universitatis Upsaliensis No. 233, Faculty of Science and Technology, Uppsala University, 2006.
- [11] L. Ballabio, et al., *Nucl. Fusion* 38 (11) (1998).
- [12] A. Hjalmarsson, et al., Characterization of a scintillator detector with charged particles and pulse light emission, Uppsala University Neutron Physics Report UU-NF 05#13, December 2005, ISSN 1401-6269, <http://www.inf.uu.se/Reports/Internal.html>.
- [13] L. Giacomelli, Development of instrumentation for neutron emission spectroscopy diagnosis of fusion plasmas in deuterium, Uppsala University Neutron Physics Report UU-NF 02#9, July 2002, ISSN:1401-6269.
- [14] J. Sousa, et al., *Fusion Eng. Des.* 71 (2004) 101.
- [15] A. Hjalmarsson, et al., Response function simulation of the TOFOR neutron time-of-flight spectrometer, Uppsala University Neutron Physics Report UU-NF 06#06, September 2006, ISSN 1401-6269, <http://www.inf.uu.se/Reports/Internal.html>.
- [16] C. Hogben, S. Griph, Interfacing to JET plant equipment using the HTTP protocol, CODAS Document Centre, <[http://w3.jet.efda.org/CODAS/Document\\_Library](http://w3.jet.efda.org/CODAS/Document_Library)>, 2002.
- [17] M. Tardocchi, et al., *Rev. Sci. Instr.* 75 (10) (2004) 3543.
- [18] E. Ronchi, A Bipolar LED drive technique for high performance, stability and power in the nanosecond time scale, *Nucl. Instr. Meth. A.*, to be submitted.
- [19] JET Final Report JW2-OEP-ENEA-21.01, Responsible Officer G. Gorini.
- [20] JET Site Inspection report JET6678, Alstec Systems Technology, 02.03.2005.
- [21] JET Site Inspection Report JET6677, Alstec Systems Technology, 02.03.2005.
- [22] M. Gatu Johnson, et al., The TOFOR neutron spectrometer for high-performance measurements of D plasma fuel ion properties, in: Proceedings of the International Workshop on Burning Plasma Diagnostics, Varenna, Italy, 24th–28th September 2007, AIP conference proceedings Vol. 988, p. 311.
- [23] C. Hellesen et al., Measurement and analysis of the neutron emission from ICRH and NB heated JET D plasmas using the TOFOR spectrometer, Uppsala University Neutron Physics Report UU-NF 07#13, August 2007, ISSN 1401-6269, <http://www.inf.uu.se/Reports/Internal.html>.